Enabling Adaptive Cloud Gaming in an Open-Source Cloud Gaming Platform

Hua-Jun Hong, Chih-Fan Hsu, Tsung-Han Tsai, Chun-Ying Huang, *Member, IEEE,* Kuan-Ta Chen, *Senior Member, IEEE,* and Cheng-Hsin Hsu, *Member, IEEE*

***Abstract*—We study the problem of optimally adapting ongoing cloud gaming sessions to maximize the gamer experience in dynamic environments. The considered problem is quite challenging because: (i) gamer experience is subjective and hard to quantify, (ii) the existing open-source cloud gaming platform does not support dynamic reconfigurations of video codecs, and (iii) the resource allocation among concurrent gamers leaves a huge room to optimize. We rigorously address these three challenges by: (i) conducting a crowdsourced user study over the live Internet for an empirical gaming experience model, (ii) enhancing the cloud gaming platform to support frame rate and bitrate adaptation on-the-fly, and (iii) proposing optimal yet efficient algorithms to maximize the overall gaming experience or ensure the fairness among gamers. We conduct extensive trace-driven simulations to demonstrate the merits of our algorithms and implementation. Our simulation results show that the proposed efficient algorithms: (i) outperform the baseline algorithms by up to 46% and 30%, (ii) run fast and scale to large (≥ 8000 gamers) problems, and (iii) achieve the user-specified optimization criteria, such as maximizing average gamer experience or maximizing the minimum gamer experience. The resulting cloud gaming platform can be leveraged by many researchers, developers, and gamers.**

***Index Terms*—Cloud gaming, real-time streaming, crowdsourcing, user study, resource allocation, optimization**

I. Introduction

CLOUDS provide abundant and elastic resources for offering various online services, and have made tremendous impacts on our daily life in many ways. Computer games, along with many other applications, have been pushed into the clouds [1] in two models: file streaming and video streaming. The first, more conservative, model leverages the clouds to distribute computer games, because modern computer games often take more than one DVD to distribute. File streaming allows gamers to start playing games after a small subset of files has been downloaded, while the remaining files are streamed in the background. File streaming allows the game developers, such as Blizzard, to reduce their costs on manufacturing the physical media, and delivering patches using the same clouds. However, all these computer games still run on gamers' computers, and thus gamers: (i) need high-end computers for good graphics effects and (ii) can only play games on the installed computers.

H.-J. Hong and C.-H. Hsu are with Department of Computer Science, National Tsing Hua University, Hsin Chu, Taiwan.

C.-F. Hsu, T.-H. Tsai, and K.-T. Chen are with Institute of Information Science, Academia Sinica, Taipei, Taiwan.

C.-Y. Huang is with Department of Computer Science and Engineering, National Taiwan Ocean University, Kee Lung, Taiwan.

This work was supported in part by the Ministry of Science and Technology of Taiwan under the grants 103-2221-E-001-023-MY2, 102-2221-E-007-062-MY3, and 103-2221-E-019-033-MY2.

The second, more aggressive, model offloads intensive computations, such as rendering, physics, and artificial intelligence, to the clouds, in order to deliver more visually-appealing effects on less powerful computers anywhere, anytime over the Internet. Using video streaming, game service providers, such as OnLive [2], GaiKai [3], and Ubitus [4], deliver instantaneous gaming experience to gamers using different client computers (including mobile devices). This is done by implementing and installing a thin client on PCs, laptops, tablets, smartphones, and set-top boxes. While the recent game-specialized cloud infrastructures [5] support both cloud gaming models, we only consider the more challenging video streaming model throughout this paper.

Delivering high-quality cloud gaming experience is challenging [6], mainly because: (i) modern computer games are mostly resource hungry, (ii) the real-time nature of games imposes stringent deadline, and (iii) gamers have high expectations on different aspects of gaming experience [7]. More specifically, gamers ask for both high-quality game scenes and low response delay, where the: (i) quality of game scenes is measured by metrics like resolutions, frame rates, fidelities, and 3D effect levels, and (ii) the response delay refers to the time difference between the time when a gamer triggers an input and the time when the client renders the corresponding effect. Concurrently achieving both high-quality scenes and fast responses consumes a huge amount of computation and network resources [8]. Our prior work [9] copes with the problem by optimally selecting the most suitable data centers for incoming gamers to maximize a configurable objective function, such as overall gaming experience. The data center selection problems are solved on a portal server, so as to optimize the gaming experience in large time scales (in the order of tenths of minutes). However, the cloud systems and network resources change in small time scales (in the order of seconds), which cannot be compensated by optimal data center selection *alone*, and thus a finer-grained adaptation mechanism is required for each game session.

In this paper, we study the problem of *adapting* cloud gaming sessions to maximize the gamer experience in dynamic systems and networks. Without adaptations, cloud gaming platforms continuously deliver the cloud games to gamers at the highest possible quality even when the resources are insufficient. This may overload the network because a large part of the network resources is consumed by the downstream traffic (game videos) [10]. Thus, the video bitrate of an ongoing cloud gaming session should be reduced if the end-to-end bandwidth is insufficient. Moreover, when the bandwidth is significantly reduced, the video frame rate may have to be reduced to maintain a satisfying graphics quality. Otherwise, gamers would suffer from degraded gaming experience due to late and lost frames, and may quit the games prematurely.

Achieving optimal adaptations is no easy task because gamers are picky, and love to have both high graphic quality and short interaction delay. However, concurrently optimizing *both* gamers' demands is impossible. Therefore, in order to solve the cloud gaming bitrate adaptation problem, we carefully study the following three main challenges:

- **Quantifying gamer experience via crowdsourcing.** The metrics of higher-level gamer experience and lower-level system performance are quite different, and the mapping between them is affected by many factors. Conducting a user study in a lab to exercise all the factors requires many participants, and is tedious and expensive. Hence, we leverage crowdsourcing for a user study with many more online participants in Section IV, and derive empirical gamer experience, or Mean Opinion Score (MOS) model. Crowdsourcing also allows us to conduct the user study using gamers' actual client computers for more realistic results, compared to user studies done in a lab.
- **Reconfiguring video codecs.** Compared to audio streams, encoding and transmitting video streams consume much more computation/network resources, and thus video codec is the main control knob for adapting an ongoing cloud gaming session to the available resources. Changing the codec configuration on-the-fly is challenging, and we report the lessons learned in Section V.
- **Adapting videos in dynamic networks.** With the gamer experience model and codec reconfiguration mechanism, we then develop a suite of techniques to quickly adapt the video codec configurations to dynamic networks. The techniques range from optimal resource allocation algorithms to real-time heuristics to maximize the gamer experience without excessive resource consumption. These techniques are presented in Section VI.

The derived models and developed techniques have to be implemented in a real cloud gaming platform to facilitate experiment-based evaluations. However, we cannot rely on the commercial cloud gaming platforms [2–4], because they are closed and proprietary. Hence, this paper is built upon GamingAnywhere (GA) [11, 12], which is an open-source cloud gaming platform designed (see Figure 1) for researchers, engineers, and gamers. The design philosophy of GA includes extensibility, portability, configurability, and openness, and thus is very suitable to cloud gaming research. At the time of writing, the GA system does not include the game portal, and we present our game portal design in this paper. The game portal hosts several optimization algorithms, including the data center selection algorithm [9] and the adaptation algorithm. The adaptation algorithm is developed in the current work, which enhances the GA system to support video codec reconfiguration in order to adapt to dynamic networks. More details on the original GA are given in [12].

More precisely, we add four software components in GA client/server, as illustrated in Figure 2, to support adaptation. *Bandwidth estimator* monitors the sending/receiving timestamps of video packets at GA client, so as to estimate the effective bandwidth[1]. GA client sends the estimated effective bandwidth to GA server, where *codec parameter selector* determines the optimal encoding bitrate and frame rate to maximize the user experience. Such decisions are made based on an *MOS model*, which converts each pair of bitrate and frame rate into a game-dependent MOS score. The optimal encoding bitrate and frame rate are sent into *codec reconfigurator* for on-the-fly video adaptation. We present the codec reconfigurator and bandwidth estimator in Section V, and the MOS model and codec parameter selector in Section VI.

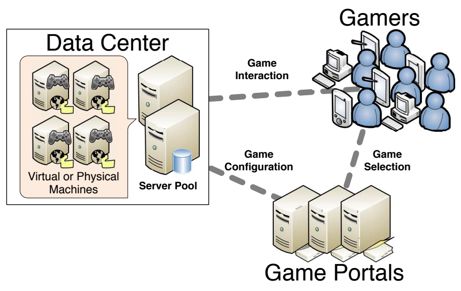

Fig. 1. The overview of cloud gaming platforms.

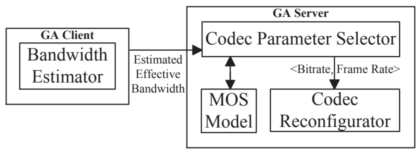

Fig. 2. The new components in the proposed adaptive cloud gaming system.

II. Related Work

A. Cloud Gaming Platforms

In cloud gaming platforms, there are several approaches to divide the tasks between the cloud servers and clients. With *graphics streaming* [13, 14], the cloud servers send all graphics commands to the clients, which then render the graphics commands using the clients' GPUs. This approach dictates more powerful GPUs to render high-quality game scenes in real time, which is less applicable for resource-limited mobile devices and set-top boxes. With *post-rendering operations* [15, 16], the 3D rendering is done at the cloud servers, and part of the post-rendering operations are done on clients. Such post-rendering operations on the clients include augmenting motions, lights, and texture [17]. This approach complicates the game development and increases the development cost, which may drive the game developers away from the cloud gaming platforms. With *video streaming* [18, 19], the cloud servers render the game scenes and stream videos to the

[1]Packet losses and delays are considered when estimating the *effective bandwidth.*

clients. The clients decode and display videos, which is a much lighter weight operation compared to the other two approaches. Comparatively, the video streaming approach: (i) demands the least resources at the clients, (ii) is easier to implement, (iii) is easier to port to heterogeneous clients, and (iv) requires the minimum augmentations on game code.

Hence, the mainstream commercial cloud gaming platforms, such as OnLive [2], GaiKai [3], and Ubitus [4], all adopt the video streaming approach. Similar approaches are taken by several cloud gaming platforms [12, 18, 19] in the literature. Among these platforms, GA [12] is open, modularized, cross-platform, and efficient. It is the first complete open-source platform of its kind. GA has been leveraged by several research projects on cloud gaming, such as mobile cloud gaming [20, 21], e-learning applications [22], GPU consolidation [23], and cloud resource allocation [9].

B. Resource Allocation in Cloud Gaming Platforms

The resource allocation problem in the clouds has been studied for some game genres. For example, Lee and Chen [24] study the resource allocation problem for Massively Multiplayer Online Role-Playing Game (MMORPG), and propose a zone-base algorithm to reduce the hardware requirements of the servers. However, these game servers handle short state update messages, and thus are different from cloud gaming servers that stream high-quality real-time videos to the clients. Duong et al. [25] and Wu et al. [26] focus on the admission control problem, to minimize the queueing delay of cloud gaming platforms. In particular, Duong et al. [25] develop algorithms to selectively admit incoming users for the highest profit, and Wu et al. [26] propose a similar algorithm to quickly serve users in the waiting queue. Wang and Dey [27] propose an adaptive algorithm to dynamically adjust the rendering parameters, such as lighting modes and texture details, to adaptively allocate resources. Cai et al. [28] study the resource allocation problem between a cloud server and a client computer. They divide a game into several software components and intelligently dispatch the components among multiple cloud servers and client computers. Our earlier works [9] consider a different problem of maximizing the gaming Quality of Experience (QoE) of all admitted users, by placing virtual machines in the best data centers under diverse network conditions, such as network delay. The current paper, in contrast, addresses the problem of dynamic adaptations in ongoing game sessions.

III. System Architecture of the Extended Cloud Gaming Platform

We extend GA for a complete cloud gaming service, and the system architecture is illustrated in Figure 3. The proposed architecture consists of four entities: a manger, portals, servers, and clients. This figure depicts the working flows among the entities with numbered steps. The manager is a logically-centralized entity running on a server or server farm, and is responsible for pointing servers to portals. Multiple portals can be deployed for the sake of scalability, although only one portal is shown in the figure for brevity. Each server is

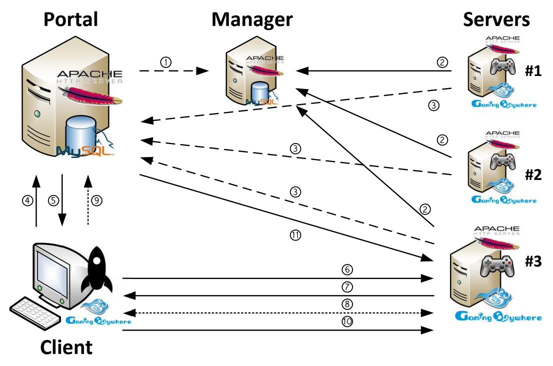

Fig. 3. The working flows among the portal, manager, servers, and clients.

associated with and managed by a portal, and the server may run on a virtual or physical machine. Heartbeat messages (not shown in the figure) are periodically exchanged between a pair of associated server and portal, in order to maintain the awareness of the existence of the other party. The server is associated with a portal as follows. When the portal is up, it registers with the manager (step 1). When the server is up, it asks the manager for available portals (step 2), and then reports to one of the available portals (step 3). After this, the server, which runs the actual game, is associated with and managed by the portal. The server repeats steps 2 and 3 if the connection to the portal is broken.

When a client attempts to use the cloud gaming service, it executes a launcher to interact with the portal (steps 4 and 5). The launcher retrieves a list of available games on the portal, lets a player select a game, and gets an available server for the selected game from the portal. Then the launcher requests the server to launch the GA server and the selected game (step 6), and downloads required client setup information from the server (step 7). Last, the launcher launches the GA client to connect to the server and starts the game play (step 8). During a game play, the launcher monitors the GA client and periodically sends a heartbeat message to the portal to indicate that the game play is still ongoing (step 9). The launcher sends a terminating signal to the server if the user quits the game (step 10). In case that the client is not shutdown normally, the portal detects the issue by missing heartbeat messages. When an abnormal shutdown is detected, the portal sends a cleanup message (step 11) to the corresponding server of the abnormal user, in order to release the resources, such as CPU, memory, and disk occupied by the client. The extended system architecture will be released to the public [11], and can be leveraged by more researchers, developers, and gamers.

IV. Quantifying Gamer Experience via Crowdsourcing

We present a crowdsourcing system built on GA, a crowdsourced user study, and several new findings.

A. Online Questionnaire System

We first design an automatic online questionnaire system to collect user experience in playing games via GA under diverse configurations. There are several proposals to quantify

TABLE I
SUMMARY OF THE CROWDSOURCED STUDY

Game	Batman, FGPX, CoD
Bitrate	0.5, 1, 2 Mbps
Frame Rate	10, 20, 30 fps
# of Subjects	101
# of Experiments	167
# of Game Sessions	3,020
Mean (std) Session Time	173 (59) seconds
Total Session Time	132.2 hours
Mean (std) Graphics Quality	4.13 (1.66)
Mean (std) Interactivity Quality	4.44 (1.50)
Mean (std) Overall Score	4.16 (1.51)

user experience in cloud gaming platforms [29–31]; interested readers are referred to the survey [31] for a complete list of these quality metrics. In this work, we adopt Mean Opinion Score (MOS), which is a subjective score from 1 (worst) to 7 (best), as the performance metric of our questionnaire system[2]. The system design is consistent with the architecture given in Figure 3. An invited participant first launches the questionnaire client using his/her computer, which connects to the portal server and shows a welcome message to describe the experiment. If the invitee agrees to participate in the experiment, he/she clicks a button to start the experiment. The questionnaire client then finds an available GA server registered on the portal, randomly picks a server configurations, launches the game on the game server, and runs the GA client for the subject to start the game play. We vary bitrate, frame rate, and game in different configurations and the details are summarized in Table I. Each game session lasts for 2–4 minutes; specifically: (i) a game needs to be played for 2 minutes before the client can be manually terminated, and (ii) the client will be forcefully terminated after 4 minutes. After a game session is finished, the questionnaire client shows an online questionnaire form for the subject to fill in. The subject then plays the same game under 8 other configurations (9 configurations in total, which are in a random order). Each subject needs to play one game (with 9 configurations), but may opt for more games (3 games in total). If a subject quits before finishing the 9 configurations for a game, his/her inputs of the gaming experience are not considered.

The questionnaire client is implemented as a Windows program with an embedded Internet Explorer object. Both the portal and GA server are wrapped as web services. The questionnaire client leverages `libcurl` to interact with the portal server and launches the selected GA server with a specific configuration. The online questionnaire form is created using Google spreadsheet and is presented to the user in the embedded Internet Explorer object. To prevent the spreadsheet from being abused by attackers or malicious users, we generate a keyed Message Authentication Code (MAC) for each game play and pre-fill it into corresponding questionnaire form.

[2]In our pilot tests, some subjects reported that it's hard to make decisions in a typical score range between 1 and 5 as the differences between the video quality in different rounds are sometimes subtle. Thus, we are suggested to increase the range of scores such that subjects can report minor differences [32]. On the other hand, the range cannot be too large as it is limited by psychometric properties of humans. Therefore, we choose the maximum suggested range of seven [32] in our questionnaires.

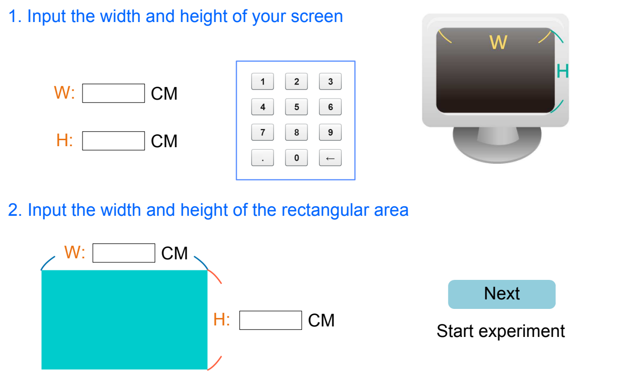
1. Input the width and height of your screen
W: CM
H: CM
1 2 3
4 5 6
7 8 9
. 0 ←
W
H
2. Input the width and height of the rectangular area
W: CM
H: CM
Next
Start experiment

Fig. 4. The instructions and interface for users to input the physical dimension of their computer monitors.

Only forms with valid keyed MACs are considered in our evaluations.

One tricky part of carrying out the crowdsourced user study is: subjects use their own home/office computers, and thus the physical monitor dimensions and display resolutions may be quite diverse. Therefore, we add an additional test to estimate the monitor characteristics as follows. We first present a user interface in full screen as illustrated in Figure 4, which asks the subject to fill in the physical dimension of the monitor. The subjects may not know the exact sizes, and thus we ask them to measure the viewable area of the monitor with rulers. To filter out erroneous information, a rectangle is displayed on the screen and the subjects are also asked to measure the size of the rectangle on their monitors with rulers. By comparing both inputs, i.e., the dimensions of the monitors and those of the rectangle, we filter out erroneous inputs and exclude these subjects from the user study. The display characteristics, including monitor size, screen resolution, and pixel density, are later analyzed to see how they affect game play experience.

B. Overall Results

We conduct the crowdsourced user study online between July and September 2014. Upon filtering out subjects who made problematic inputs (such as all the ratings for all the configurations are consistently 1 or 7), we end up with 101 subjects and 167 experiments. Among the subjects, 51% of them are females and 49% are males; the ages of subjects are on average 27 years old with a standard deviation of 5.5 years (ranging from 19 to 41 years old); 30% of them are students and the remaining subjects have diverse professions, including salesperson, accountant, government officer, and so on. The subjects have quite diverse experience in computer game play, as their gaming history spans from 4 to 34 years (with an average of 12 years); in addition, they are also dissimilar in terms of the average time spent in computer gaming per day: The daily game play time ranges from 15 minutes to 6 hours with an average and standard deviation of 2 and 1.5 hours respectively. These figures indicate that our subjects are from different background; thus, though the number of subjects is not significantly large, but they should constitute of a relatively representative sample of the Internet

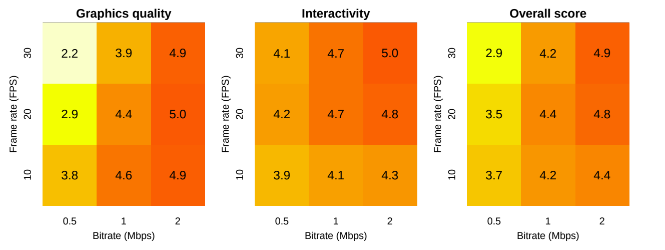

Fig. 5. Aggregated MOS scores under different configurations (bitrate and frame rate).

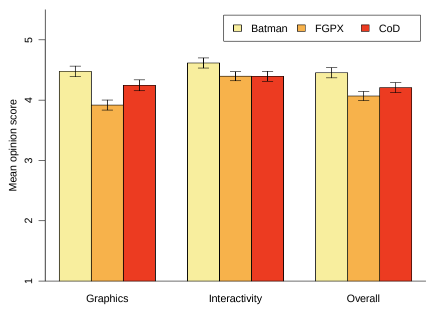

Fig. 6. Impacts of games on aggregated MOS scores.

users. The overall statistics of the dataset we collected from the experiments are summarized in Table I.

We first compute the aggregated MOS scores under different bitrates and frame rates, and plot them in Figure 5 with several observations. First, when the frame rate is fixed, higher bitrates always result in higher MOS scores, demonstrating the importance of allocating the available bandwidth among gamers. Second, higher frame rates lead to lower graphics quality, because higher frame rates essentially mean more video frames to encode. Third, higher frame rates result in higher interactivity, because the games are more responsive. Fourth, and most interesting, when the bitrate is high (2 Mbps), higher frame rates lead to better overall scores; when the bitrate is low (0.5 Mbps), higher frame rates lead to lower overall scores. Such difference may be attributed to the *already* inferior graphics quality when bitrate is low: further degradation on graphics quality due to higher frame rates is not acceptable. This finding reveals that *increasing frame rates not necessarily improves overall MOS scores,* and therefore carefully choosing the best configuration is critical.

C. Impacts of Games on MOS Scores

Next, we study the implication of different games on MOS scores. The three considered games are from different game genres. Lego Batman (Batman) is a 3D adventure game, Sin Cyber Grandprix 2 (FGPX) is a car racing game, and CoD: Modern Warfare 2 (CoD) is a first-person shooter game. Among the three games, Batman's game screens consist of rendered cartoon characters and are easier to compress. The game screens of CoD and FGPX are more complex and they are in faster pace (especially FGPX). Such difference can be observed in the per-game overall MOS scores reported in Figure 6. First, in terms of graphics quality, Batman outperforms CoD, which in turn outperforms FGPX. This can be attributed to the less complicated game screens in Batman, and faster game screen changes in FGPX. Second, in terms of interactivity, subjects are less picky to the slower-pace Batman. Last, the overall scores show similar trends as the graphics quality and interactivity scores.

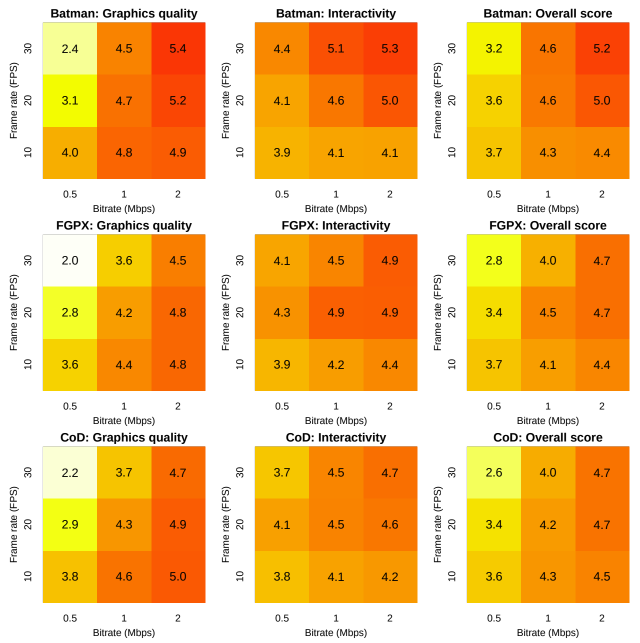

Fig. 7. Detailed per-game MOS scores under different configurations (bitrate and frame rate).

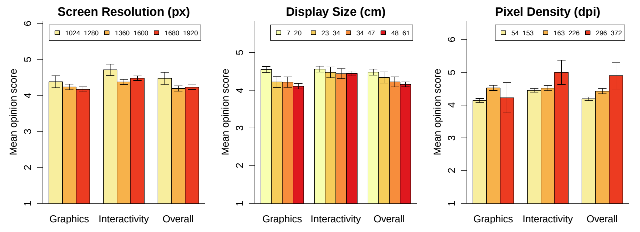

Fig. 8. Impacts of display settings on overall MOS scores.

Next, we plot the per-game MOS scores under different configurations in Figure 7, which leads to important observations. First, across the considered games, we see consistent pattern, similar to the aggregated MOS scores reported in Figure 5. Second, and more importantly, under the same configuration, subjects playing different games report different MOS scores. This observation, along with earlier ones, concludes that the MOS scores depend on bitrate, frame rate, and game. We use the detailed user study results to derive an empirical MOS model in Section VI, which is used to estimate the gaming experience under different configurations.

D. Impacts of Display Settings on MOS Scores

We also report the implication of the display settings on the overall MOS scores in Figure 8. First, higher screen resolutions result in lower MOS scores. This is counter-intuitive as it is a common belief that higher resolutions result in better

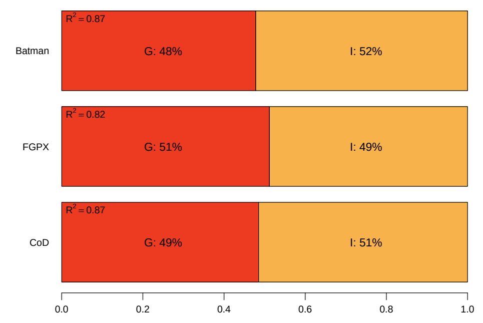

Fig. 9. Decomposition of overall MOS scores on games.

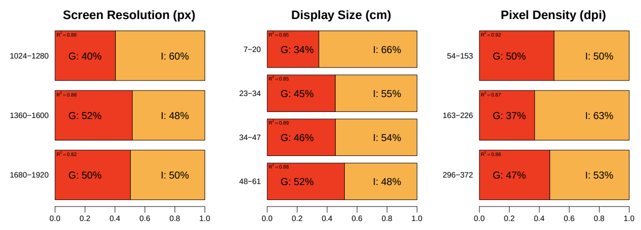

Fig. 10. Decomposition of overall MOS scores on display settings.

user experience. We attribute this observation to the tendency of subjects to *deduct* MOS scores when *seeing flaws* [33]; in other words, higher resolutions amplify the imperfection if any. Second, larger display sizes also result in worse MOS scores, which can also be attributed to the amplified imperfection. Last, if we normalize the screen resolution and display size into pixel density, we find that higher pixel densities result in better interactivity and overall MOS scores. However, the graphics quality suffers when the pixel density is very low ($\leq$ 153 dpi) or very high ($\geq$ 296 dpi). To the best of our knowledge, such observation on cloud gaming platforms has not been made in other user studies.

E. Decomposition of Overall Scores

Last, we study the mapping among the graphics quality, interactivity, and overall scores. We find that the overall scores can be written as a weighted linear function of those of graphics quality and interactivity scores. Figure 9 reports the overall decomposition for individual games, with adjusted R^2 values annotated. This figure shows that the graphics quality and interactivity are approximately equally important for all games. FGPX, as a fast-pace game with complex game screens, leans toward the graphics quality a bit, but the difference is minor.

However, the variation in overall score decomposition is significant if we consider the effect of display settings, which we plot in Figure 10. This figure reveals that higher resolutions and larger display sizes lead to more weights on the graphics quality scores. This is consistent with our observations made in Figure 8: the imperfection is easier to be noticed by the subjects under higher screen resolutions and larger display sizes. In addition, Figure 10 also shows that when the pixel density is low or high, the subjects are more sensitive to the graphics quality.

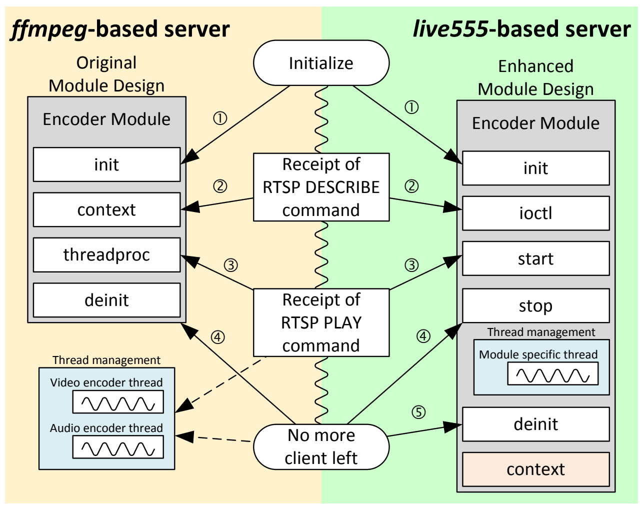

Fig. 11. Comparison between the original and the enhanced module designs.

V. Reconfiguring Video Codecs in Run Time

We enhance GA to support dynamic video codec reconfigurations. The improvement covers several aspects, which are elaborated in this section.

A. Migration from ffmpeg to live555

We replace *ffmpeg*, which supports several codecs and RTSP/RTP features, with *live555* for three major reasons: (i) It is difficult to add a customized codec into the complicated *ffmpeg*. (ii) Using *ffmpeg* cannot dynamically reconfigure video codecs. (iii) The RTP feature provided by *ffmpeg* is tightly coupled with its implementation. Hence, making a customized non-*ffmpeg* codec to work with *ffmpeg*'s RTP stack is not easy.

Unlike *ffmpeg*, *live555* has a built-in RTSP server implementation. We can use the *RTSPServer* class to create an RTSP server object instead of implementing it on our own. However, we need to create our own RTSP sub-sessions for audio and video streams and provide corresponding live audio and video sources. Our current *live555*-based implementation supports a number of codecs, namely, MP3, AC3, OPUS (audio codecs) and H.264, H.265, VP8 (video codecs). Moreover, *live555* offers a more comprehensive RTCP implementation, which allows us to measure and collect the network statistics, including packet loss rate, bitrate, round-trip time, and jitter. These numbers can be used as inputs for optimization algorithms. *Live555* still achieves comparable performance than the *ffmpeg*-based GA in terms of game playing latency.

B. Enhanced Module Design

Figure 11 compares the original and the enhanced module design. The left half of Figure 11 shows the working flow of the *ffmpeg*-based server. The encoder module provides an interface to the server to retrieve its corresponding codec context. A codec context is used to generate a SDP (session description protocol) description, which contains the detailed configuration for an RTP session, including the adopted codec and associated codec parameters. In addition, the original design leaves the management of encoder threads in the RTSP server. Consequently, the server has to create corresponding encoder threads, and terminate any running encoder threads when no clients are connected. Leaving thread management at the server complicates the implementation of the RTSP server.

The right half of Figure 11 shows the working flow of the *live555*-based server. In order to loose the tight relationship between the server and the modules, we add a new *ioctl* interface for GA modules. Therefore, all the GA components are able to interact with a module using the *ioctl* interface. With the new design, the server now retrieves the required SDP parameters via the *ioctl* interface on receipt of a RTSP DESCRIBE command. Moreover, the generic *ioctl* interface also simplifies the task for codec reconfiguration.

C. Codec Reconfiguration

On top of the revised architecture, we implement three H.264 encoder modules that support dynamic codec reconfiguration. One is software-based implemented with *libx264* and the other two are hardware-based. The hardware-based codecs work with the Video Processing Unit (VPU) on Freescale's ARM-based i.MX6 CPU and the Quick Sync Video (QSV) technology on Intel's HD Graphics and recent Intel CPUs.

Software-based module. The software-based module is highly flexible to reconfigure the codec *anytime* using *x264_encoder_reconfig* function. *libx264* provides three rate control modes: ABR, CRF, and CQP. The ABR mode generates video streams at a given average bitrate, but the bitrate *cannot* be changed once the encoder is initialized. Hence, we stick with either the CRF or the CQP modes, configured via the `crf` and `qp` parameters, respectively. The generated video bitrate using CRF and CQP largely depends on the complexity of a frame and the degree of changes between adjacent frames. We can nevertheless limit the maximum bitrate by specifying *both* the `vbv-maxrate` and `vbv-bufsize` parameters. To understand the effect of the CRF parameter, we measured the relationship between the CRF parameter and the bitrate of the generated video stream. In the experiments, we stream a 720P music video at different frame rates from a GA server to a client over a wireless network. The valid CRF value ranges from 0 (lossless) to 51 (very lossy), where a lower CRF value generates a better quality video in principle. Since we are working with H.264's main profile, the minimum valid CRF value is 1 and the default CRF value adopted by *libx264* is 23. Table II shows that when the `vbv-maxrate` parameter is *much lower* than the required CRF setting, some mosaic blocks appear on video frames while the rest part of the frames is clear. This may be because the rate control algorithm runs out of the available bits specified by `vbv-maxrate` in the middle of encoding a frame, it has to switch to low-quality configurations for un-encoded parts. Such quality degradations happen when the two parameters (i.e., CRF and `vbv-maxrate`) are largely mismatched, which indicates that a careful tuning of such parameters is required.

TABLE II
MEASURED BITRATE UNDER VARIOUS CRF SETTINGS

		Measured bitrate		Measured frame loss rate		
Frame rate	CRF	Min	Max	Min	Max	Avg.
24	1	2.5Mbps	36Mbps	0%	0%	0%
	12	2.2Mbps	12Mbps	0%	0%	0%
	23	1.3Mbps	4.1Mbps	0%	0%	0%
	37	600Kbps	1.1Mbps	0%	0%	0%
	51	150Kbps	450Kbps	0%	0%	0%
30	1	2.9Mbps	41Mbps	0%	0%	0%
	12	2.6Mbps	13Mbps	0%	0%	0%
	23	1.6Mbps	4.5Mbps	0%	0%	0%
	37	750Kbps	1.2Mbps	0%	0%	0%
	51	169Kbps	476Kbps	0%	0%	0%
50	1	4.9Mbps	43Mbps	0%	34.49%	10.19%
	12	4.0Mbps	16Mbps	0%	0.42%	0.12%
	23	2.3Mbps	5.4Mbps	0%	0.23%	0.04%
	37	991Kbps	1.5Mbps	0%	0.12%	0.0003%
	51	221Kbps	602Kbps	0%	0.13%	0.0000%

Hardware-based module. The other two hardware-based encoder modules are based on VPU and QSV technologies, respectively. They generally achieve shorter encoding latencies and incur lower CPU loads than software-based modules. However, such efficiency may sacrifice the flexibility.

The VPU implementation supports H.264 hardware codecs with the baseline, main, and high profiles. VPU requires the YUV420 format and supports the dynamic reconfiguration of the bitrate, frame rate, GOP number, and slice mode, via the *vpu_EncGiveCommand* API. Such reconfiguration can be done in either the frame level or the macroblock level.

The QSV implementation supports several hardware-based codecs. Meanwhile, they provide quite a few Video Pre-Processing (VPP) operations, such as color space conversion, resizing, and de-interlacing. The encoders provided by QSV only support the NV12 pixel format; thus we use its VPP feature to convert the original pixel format of the source frames to NV12. QSV also supports codec reconfiguration in run time, but it is less flexible. From its SDK reference manual, it supports at least the run-time reconfiguration of the video bitrate without resetting an encoder. In case an encoding parameter cannot be dynamically reconfigured, the encoder will be reset. QSV supports several rate control modes, including CBR, VBR, CQP, and AVBR. If the bitrate capping is required, one can choose CBR, VBR, or AVBR mode. In CBR and AVBR mode, only the target bitrate (*TargetKbps*) can be reconfigured, where both the target bitrate and max bitrate (*MaxKbps*) can be reconfigured in VBR mode at run time. We have integrated both hardware encoders into GA.

D. Effective Bandwidth Estimation

We implement a bandwidth estimator inspired by WBest [34] to estimate the effective bandwidth. Different from other proposals [34–36], we leverage existing video packets for effective bandwidth estimation, without incurring network overhead. We can do this for two reasons: (i) the workload of sending video packets is high (for 30-fps videos, we send a frame every 33 ms) and (ii) the size of a video frame is typically higher than MSS (Maximum Segment Size), so each video frame is split into multiple back-to-back packets. Our bandwidth estimator keeps track of the dispersion time of the video packets. To cope with fluctuations, we select the median value as the estimated capacity from every W packets. We then send video packets at the estimated capacity to measure the effective bandwidth with W video packets. The value of W is empirically selected by experiments, and we consider $W \in \{100, 200, 300, 400, 500\}$. The estimation accuracy with $W = 100$ is 50% in the worst case. In other cases ($200 \leq W \leq 500$), the accuracy is as high as 80+% and the differences among different W values are smaller than 5%. Hence, we let $W = 200$ as default for shorter reaction time.

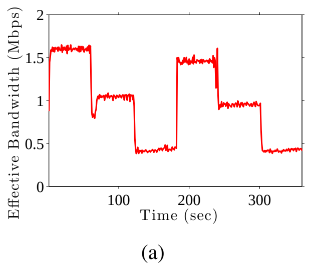

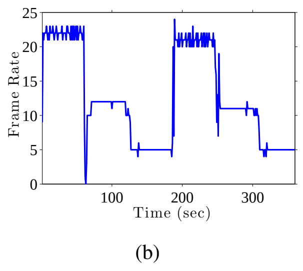

Fig. 12. The measured: (a) effective bandwidth and (b) frame rate.

E. Experiments on a Real Testbed

We conduct real experiments to show the effectiveness of our reconfiguration feature. We set up a testbed with a GA server and a GA client, and connect them via a Dummynet box. GA's off-the-shelf video codecs allow us to adaptively reconfigure video *bitrate* and *frame rate*. The bitrate is reconfigured to be the estimated effective bandwidth and the frame rate is chosen using Eq. (4) in Section VI.

Next, we evaluate the adaptive GA platform running CoD as follows. We write a script on the Dummynet box to repeatedly switch the bandwidth among 2048, 1024, and 512 kbps once every 60 secs. We then adaptively reconfigure the video bitrate and frame rate. Figure 12(a) reveals that our bandwidth estimator successfully detects the bandwidth changes. Figure 12(b) shows that the codec parameter selector quickly recovers from sudden frame rate drops due to throttled bandwidth, by adjusting the video coding parameters (bitrate and frame rate). Our experiments demonstrate how our cloud gaming platform adapts to network dynamics for a single gamer. We consider the adaptation problem across multiple gamers sharing a bottleneck link in the next section.

VI. Adapting Videos of Multiple Gamers in Dynamic Networks

We solve the resource allocation problem among multiple gamers. Our proposed algorithm runs on the portal server.

A. Notations and Model

We consider a data center serving U gamers as illustrated in Figure 13, where each gamer is connected to a GA server. All U GA servers share an outgoing link of the data center, and we let R be the current available link bandwidth. The value of R is fluctuating due to the background traffic, and we employ Exponentially Weighted Moving Average (EWMA), or similar techniques, to estimate the R value. We let f ($1 \leq f \leq F$) and b ($1 \leq b \leq B$) be frame rate and bitrate, respectively and they are specified by the system administrators. We let g ($1 \leq g \leq G$) be the game supported by the cloud gaming platform, and p_u be the game played by gamer u, where $1 \leq u \leq U$ and $1 \leq p_u \leq G$. We let $m_{g,f,b}$ be the MOS score of playing game g at frame rate f and bitrate b, which can be derived via off-line user studies or online regression.

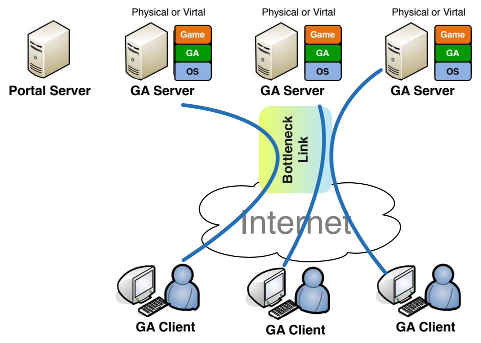

Fig. 13. Adapting videos of GA servers in a data center.

For concrete discussions, we adopt the user study reported in Section IV-C in general, and in Figure 7 in specific, to empirically model the MOS scores. We note that our MOS model is designed to drive the codec reconfiguration decisions at the GA server, rather than estimate the actual user experience at the GA client. The MOS model implicitly considers the available bandwidth, and ignores the network latency. This is because the network latency is not controllable by GA server/client during ongoing cloud gaming sessions. When a game session is affected by higher packet loss rate or longer end-to-end delay, our bandwidth estimator (Section V-D) reports lower effective bandwidth. Then, the codec parameter selector picks a new target bitrate (as a function of effective bandwidth), using the MOS model that converts the bitrate and frame rate into the expected MOS score. Different from our MOS model, there are full-fledged QoE models in the literature for precise user experience. For example, Game Mean Opinion Score (GMOS) [29–31] is an objective quality metric, which is a function of codec, frame rate, resolution, PSNR (Peak Signal-to-Noise Ratio), network latency, and packet loss rate. Compared to our simple MOS model, GMOS is too complicated for video codec reconfiguration purpose. More importantly, the additional complexity comes from factors that are not directly controllable by the GA server/client.

We tried several popular functions, and decided to use the following quadratic MOS model:

$$m(g, f, b) = \alpha_{g,1} f + \alpha_{g,2} b + \alpha_{g,3} f^2 + \alpha_{g,4} b^2 + \alpha_{g,5} fb + \alpha_{g,6}, \tag{1}$$

where $\alpha_{g,1}$–$\alpha_{g,6}$ are game-specific model parameters. The goodness-of-fit statistics are summarized in Table III, which demonstrates that the model closely follows the results of our user study. The derived models are visualized in Figure 14, which are consistent with the ground-truth reported in Figure 7. We note that, deriving the model parameters may not be

TABLE III
THE MOS MODELS FOR INDIVIDUAL GAMES

	Batman	FGPX	CoD
	(1)	(2)	(3)
fps, $\alpha_{g,1}$	0.010 (0.036)	0.038 (0.041)	−0.011 (0.037)
rate (Mbps), $\alpha_{g,2}$	2.940*** (0.484)	2.297** (0.553)	2.529** (0.491)
I(fps^2), $\alpha_{g,3}$	−0.001 (0.001)	−0.002 (0.001)	−0.001 (0.001)
I(rate^2), $\alpha_{g,4}$	−1.150*** (0.176)	−0.868** (0.201)	−0.939** (0.178)
fps:rate, $\alpha_{g,5}$	0.043** (0.008)	0.036** (0.009)	0.037** (0.008)
Constant, $\alpha_{g,6}$	2.248** (0.428)	2.369** (0.490)	2.621*** (0.434)
R^2	0.988	0.981	0.987
Adjusted R^2	0.968	0.949	0.966
F Stat. (df = 5; 3)	49.518***	31.040***	46.130***

Note: *p<0.1; **p<0.05; ***p<0.01

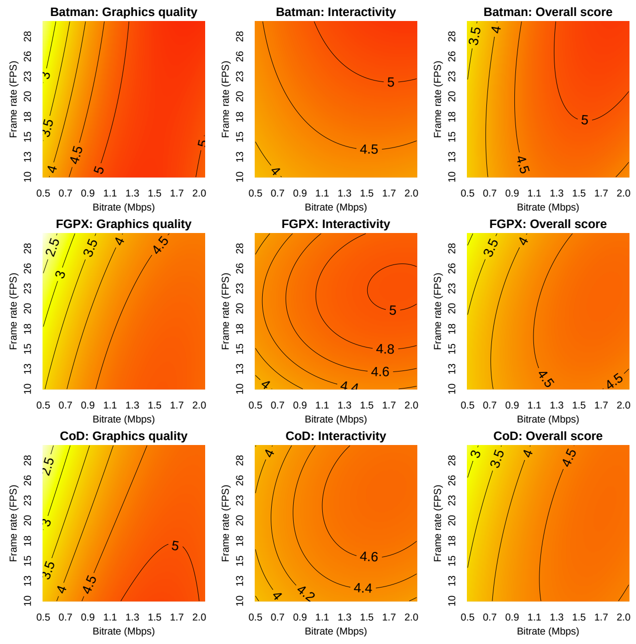

Fig. 14. Illustration of the resulting per-game QoE models.

trivial, and there are a number of ways to ease the burden. For example, one may classify the computer games into a few genres such that games in the same genre share similar video and game play characteristics or therefore are similarly *friendly* to cloud gaming QoE [7]. In addition, a service provider can continuously and probabilistically collects users' experience ratings via simple questions to derive game-specific models. Such post-session questionnaires are frequently adopted by various online services.

Next, we let $\hat{k}_u$ and $\check{k}_u$ be the maximal and minimal bitrates of gamer u, respectively. The minimal $\check{k}_u$ is assigned by the system administrator based on some practical concerns. For example, a rule-of-thumb may indicate any bitrates less than 50 kbps do not produce meaningful reconstructed videos, leading to $\check{k}_u = 50$ kbps. $\hat{k}_u$, on the other hand, comes from a common property of hybrid video coders: the video quality saturates when the bitrate is increased [37]. Hence, it yields less significant improvements while the bitrate is increased beyond, e.g., $\hat{k}_u = 5$ Mbps. Moreover, the gamer's access link may be narrow and shared by multiple users/applications, leading to a bandwidth limitation on u's access link. $\hat{k}_u$ is also used to accommodate this bandwidth limit: the administrator can set $\hat{k}_u$ to be the minimum between the link bandwidth limitation and the quality-saturating bitrate, so that the allocated bitrate to u will not be wasted.

B. Problem Statement

Our adaptation problem is to select the best frame rate and bitrate for each gamer, in order to maximize the overall gaming quality under the bandwidth constraints. We consider two optimization criteria: (i) maximizing the average MOS score and (ii) maximizing the minimum MOS score across all gamers. We refer to these two optimization problems as: (i) quality-maximization and (ii) quality-fairness problems, respectively throughout this article. We let x_u and y_u ($\forall\ 1 \le u \le U$) be the decision variables, where $1 \le x_u \le F$ (frame rate) and $1 \le y_u \le B$ (bitrate). With the defined notations, we write our problem with the quality-maximization objective as:

$$maximize \sum_{u=1}^{U} m_{p_u, x_u, y_u} \tag{2a}$$

$$s.t.: \sum_{u=1}^{U} y_u \le R; \tag{2b}$$

$$\check{k}_{u'} \le y_{u'} \le \hat{k}_{u'},\ \forall\ 1 \le u' \le U; \tag{2c}$$

$$1 \le x_u \le F, 1 \le y_u \le B,\ \forall\ 1 \le u \le U. \tag{2d}$$

For the quality-fairness objective, we replace Eq. (2a) with:

$$maximize \min_{u=1}^{U} m_{p_u, x_u, y_u}. \tag{3}$$

The optimization problems are solved periodically, say once every T seconds in order to accommodate to the system and network dynamics. In the next two sections, we present optimal and efficient algorithms to solve the problems.

C. Optimal Algorithms

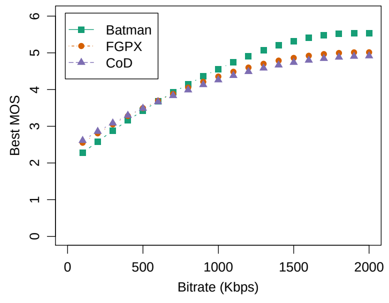

Fig. 15. The best MOS scores under different bitrates.

Solving the quality-maximization and quality-fairness problems is challenging due to the complex relations among the frame rates, bitrates, games, and MOS scores. The problems can be solved using commercial problem solvers, such as CPLEX [38]. The CPLEX comes with two solvers: the CPLEX solver and the CP solver. In our problems, because of the *min(imum)* operation in Eq. (3), we have to use the CP solver.

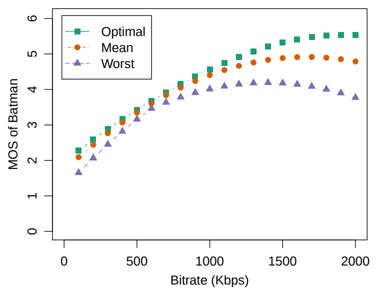

(a)

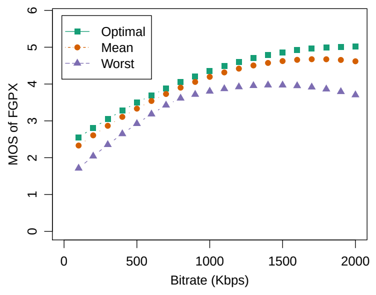

(b)

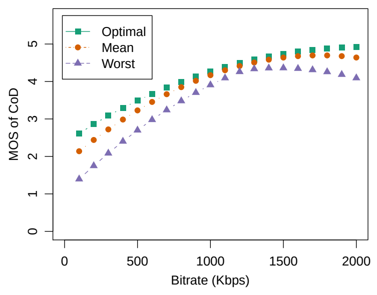

(c)

Fig. 16. Benefits of choosing optimal frame rate of different games: (a) Batman, (b) FGPX, and (c) CoD.

We refer to the CPLEX based algorithms for the quality-maximization and quality-fairness problems as OPT$_{avg}$ and OPT$_{mm}$, respectively.

D. Efficient Algorithms

While the OPT$_{avg}$ and OPT$_{mm}$ algorithms give the optimal bitrate allocation, they suffer from exponential running time, and are not suitable to real-time systems like cloud gaming platforms. Next, we develop two efficient algorithms. The intuition behind the efficient algorithms is iteratively allocating some bandwidth to the gamer that can boost the objective function value the most. Given that we iteratively *add* more bitrate to each gamer, the bitrate of any gamer is known at each step. By taking the partial derivative of Eq. (1) with respect to f, we have the optimal frame rate as:

$$f^*(b,g) = \frac{-(\alpha_{g,1} + \alpha_{g,5}b)}{2\alpha_{g,3}}, \tag{4}$$

which selects the optimal coding parameter for a gamer playing game g at the accumulated bitrate b. Next, we write the MOS scores under $f^*(b,g)$ as $mos^*(g,b)$, where:

$$\begin{aligned} mos^*(g,b) =& \alpha_{g,1}f^*(g,b) + \alpha_{g,2}b + \alpha_{g,3}(f^*(g,b))^2 \\ &+\alpha_{g,4}b^2 + \alpha_{g,5}f^*(g,b)b + \alpha_{g,6}. \end{aligned} \tag{5}$$

We plot the best MOS scores $mos^*(g,b)$ derived from the model parameters (given in Table III) in Figure 15. This figure shows that $mos^*(g,b)$ curves are monotonically increasing and saturate at $\sim$ 2 Mbps. We also plot the optimal, mean, and worst MOS scores of different games in Figure 16. This figure reports that how much benefit we can get when choosing the bitrates using Eq. (4). The gaps between the optimal and the worst MOS scores in Batman, FGPX, and CoD are up to 1.885, 1.410, and 1.122, respectively. Such gaps are nontrivial, and thus show the effectiveness of our approach.

Using Eqs. (4) and (5), we essentially transform the problem of choosing the best x_u (frame rate) and y_u (bitrate) into selecting the best y_u. For the efficient algorithms, we start from setting $\hat{y_u} = \check{k}_u$ for all $1 \leq u \leq U$, and iteratively add bitrate to the gamer that needs additional bitrate the most. We let w be the unit of allocating additional bitrate, and set $w = 1$ kbps if not otherwise specified. At each step, we define an MOS score improvement function c_u as:

$$c_u = mos^*(p_u, \hat{y_u} + w) - mos^*(p_u, \hat{y_u}), \tag{6}$$

which quantifies the benefits of investigating bandwidth w to gamer u. We also use $\hat{R}$ to denote the residue bandwidth on the bottleneck link.

For the quality-maximization problem, we iteratively allocate w to the gamer with the highest MOS improvement c_u that has not exceeded the bandwidth limitation and quality-saturating bitrate (Eq. (2c)). More specifically, we first put all U gamers in a heap sorted on their c_u in the descending order. We then follow this order to allocate the residue bandwidth until we reach the limitation of the constraint $\sum_{u=1}^{U} \hat{y_u} \leq R$. The pseudocode of our proposed EFF$_{avg}$ is given in Figure 17. For the quality-fairness problem, we iteratively allocate w to the gamer playing with the lowest MOS score. More specifically, we first put all the gamers in a heap sorted on their current MOS scores $mos^*(p_u, \hat{y_u})$ in the ascending order. We then follow the order to allocate w to gamer u, as long as the allocation does not violate the limitation of the constraint $\sum_{u=1}^{U} \hat{y_u} \leq R$. The pseudocode of our proposed EFF$_{mm}$ is given in Figure 18.

```
1:  let $\hat{R} = R$
2:  store gamers in a heap on quality improvement $c_u(\cdot)$ in the dsc. order
3:  while $\hat{R} > 0$ do
4:      pop and remove the gamer $u$ with the maximal $c_u(\cdot)$ from the heap
5:      if allocating $\hat{y_u} + w$ on $u$ satisfies (2c) then
6:          let $\hat{y_u} = \hat{y_u} + w$
7:          let $\hat{R} = \hat{R} - w$
8:          insert the gamer $u$ to the heap
9:      else
10:         remove gamer $u$ from the heap
11: let $y_u^* = \hat{y_u}\ \forall\ 1 \leq u \leq U$
12: return all $y_u^*$
```

Fig. 17. The pseudocode of the EFF$_{avg}$ algorithm.

Lemma 1 (Optimality of EFF$_{mm}$). *The EFF$_{mm}$ algorithm produces optimal bitrate allocation.*

Proof. The EFF$_{mm}$ algorithm always allocates residue bandwidth w to gamer u with the lowest MOS score at each step. Consider any alternative allocation of w to a gamer $u' \neq u$. We note that adding w to $y_{u'}$ does not improve the objective function value in Eq. (3). Compared to allocating w to u, this alternative allocation must be followed by allocating another

```
1: let $\hat{R} = R$
2: store gamers in heap on MOS scores $mos^*(\cdot)$ in the asc. order
3: while $\hat{R} > 0$ do
4:     pop and remove the gamer $u$ with the minimal $mos^*(p_u, \hat{y_u})$ from the heap
5:     if allocating $\hat{y_u} + w$ on $u$ satisfies (2c) then
6:         let $\hat{y_u} = \hat{y_u} + w$
7:         let $\hat{R} = \hat{R} - w$
8:         insert the gamer $u$ to the heap
9:     else
10:        remove gamer $u$ from the heap
11: let $y_u^* = \hat{y_u}\ \forall\ 1 \leq u \leq U$
12: return all $y_u^*$
```

Fig. 18. The pseudocode of the EFF$_{mm}$ algorithm.

w bandwidth to u to reach the same objective function value, as gamer u is the gamer with the lowest MOS score. Hence, no alternative allocation can lead to better solution when $\hat{R} = 0$. This yields the lemma. □

Lemma 2 (Optimality of EFF$_{avg}$)**.** *The EFF$_{avg}$ algorithm produces optimal bitrate allocation if the slope of $mos^*(g, b)$ monotonically decreases when the bitrate is increased.*

Proof. The MOS score improvement c_u defined in Eq. (6) is proportional to the slope. Since EFF$_{avg}$ allocates residue bandwidth to the gamer with the highest c_u, the algorithm always finds the steepest slope at the current step (locally) and across all future steps (globally). This yields the lemma. □

Next, we check whether the slope of $mos^*(g, b)$ is monotonically decreasing under the empirically-derived model parameters. First, we take double derivative of $mos^*(g, b)$ in Eq. (5), which leads to:

$$mos^*(g, b)'' = 2\alpha_{g,4} - \alpha_{g,5}^2 / 2\alpha_{g,3}. \tag{7}$$

$mos^*(g, b)$ is monotonically decreasing if the value of this equation is negative. The model parameters in Table III satisfy the condition. Hence EFF$_{avg}$ is optimal.

Lemma 3 (Time Complexity)**.** *The EFF$_{avg}$ and EFF$_{mm}$ algorithms terminate in polynomial time.*

Proof. We first create the max heap and min heap for EFF$_{avg}$ and EFF$_{mm}$, respectively. For the outer loop, we go through all residue bandwidth $\hat{R}$. We also make sure that in each iteration, the value of $\hat{R}$ is decreased at least w kbps, which is a small integer. Hence, the complexity of the outer loop is $O(R)$. Inside the loop, we first pop and remove the first gamer. In this step, the time complexity is $O(log(U))$. Next, we check the condition and try to modify the bitrate of the gamer u. If the bitrate is changed, we insert u to the heap and decrease the value of $\hat{R}$, which also costs $O(log(U))$. Hence, the complexity of the two efficient algorithms is $O(Rlog(U))$. □

VII. Evaluations

A. Setup

We build our simulator using Java and implement the proposed efficient algorithms in the simulator. For comparisons, we also implement two baseline adaptation algorithms called Base$_{eq}$ and Base$_{norm}$. The Base$_{eq}$ algorithm equally allocates the available network resources to the gamers. Base$_{norm}$ algorithm allocates the available network resources to gamers proportional to the average MOS scores of the games played by individual gamers (cf. Figure 7). For example, the overall MOS score of Batman is higher, and Base$_{norm}$ allocates more network resources to Batman for better overall MOS scores. For brevity, Base$_{eq}$ and Base$_{norm}$ set the frame rate to be 30 fps if not otherwise specified.

For realistic simulations, we drive the simulator using real traces. Each new gamer u is randomly assigned a bandwidth $\hat{k}_u$ based on the worldwide bandwidth dataset collected between January and October 2014 [39]. Each gamer also randomly selects a game from Batman, FGPX, and CoD. We use Amazon EC2 and PlanetLab nodes to collect traces of data center bandwidth R. We create an EC2 instance in Virginia, and select four PlanetLab nodes at the US East Coast. We use `iperf` to measure the bandwidth from the EC2 to each PlanetLab node once every 15 minutes for a whole day on October 12, 2014. Then, for each sample, we pick the maximal bandwidth across all four nodes, and use it as the data center bandwidth R. The average R over the 96 samples is 760 Mbps.

simulator to solve the adaptation problem once every $T = 60$ seconds if not otherwise specified. We vary the number of gamers $U \in \{250, 500, 1000, 2000, 4000\}$. We run the simulations on a PC with a 2.8 GHz i7 processor and 16 GB memory. The considered metrics are:

- *MOS:* the overall MOS score. We report both average MOS scores across all gamers, and the worst MOS scores among them. They align with objective functions of the quality-maximization and quality-fairness problems.
- *Bitrate:* the bitrate consumed by each gaming session.
- *Efficiency:* the ratio between the MOS score over the consumed bandwidth in Mbps.
- *Running time:* the execution time of each run of the adaptation algorithms.

In the next section, we report average results with 95% confidence intervals whenever applicable.

TABLE IV
MOS Scores of the Efficient and Optimal Algorithms

# of Gamers	**OPT**$_{avg}$	**EFF**$_{avg}$	# of Gamers	**OPT**$_{mm}$	**EFF**$_{mm}$
	Mean	Mean		Worst	Worst
100	5.16	5.16	1	5.53	5.53
200	5.15	5.15	2	5.01	5.01
400	5.15	5.15	4	4.91	4.91
800	4.49	4.49	8	4.91	4.91

TABLE V
Running Time of the Efficient and Optimal Algorithms (s)

# of Gamers	**OPT**$_{avg}$		**EFF**$_{avg}$		# of Gamers	**OPT**$_{mm}$		**EFF**$_{mm}$	
	Mean	Max	Mean	Max		Mean	Max	Mean	Max
100	0.02	0.03	0.090	0.097	1	0.02	0.01	0.009	0.009
200	0.15	0.16	0.102	0.103	2	0.36	0.37	0.015	0.016
400	0.95	0.96	0.153	0.157	4	4.47	4.48	0.022	0.023
800	5.01	5.02	0.237	0.248	8	125.8	127.1	0.029	0.029

B. Results

Comparisons between the optimal and efficient algorithms. We first compare the efficient algorithms against

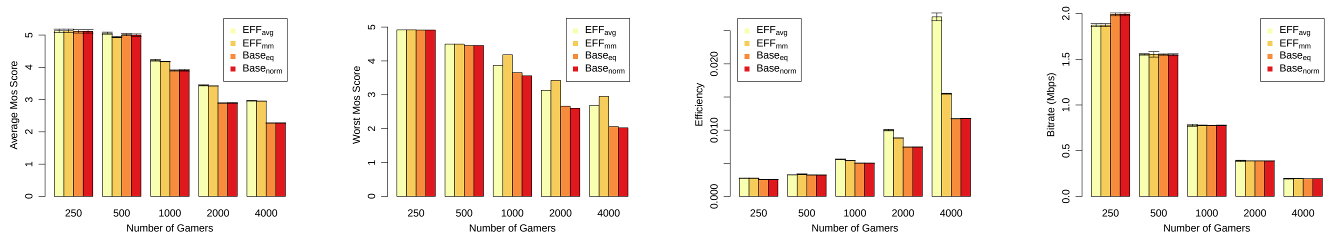
(a) (b) (c) (d)

Fig. 19. Performance of different algorithms: (a) mean MOS scores, (b) worst MOS scores, (c) overall efficiency, and (d) allocated average bitrate per gamer.

the optimal ones. Invoking OPT$_{avg}$ and OPT$_{mm}$ potentially takes prohibitively long time, and thus we set $U \in \{100, 200, 400, 800\}$ and $U \in \{1, 2, 4, 8\}$ for OPT$_{avg}$ and OPT$_{mm}$, respectively. We run each setting for a day and report the average MOS scores and running time in Tables IV and V. Table IV shows that our proposed efficient algorithms indeed produce the optimal adaptations, as proved in Lemmas 1 and 2. Table V reveals that the efficient algorithms run much faster than the optimal ones: more than 21 and 4337 times of running time reductions are observed. The running time gap is going to be even bigger with more gamers, as EFF$_{avg}$ and EFF$_{mm}$ run in polynomial time, but OPT$_{avg}$ and OPT$_{mm}$ do not. Given that the efficient algorithms achieve the optimal adaptations in polynomial time, we no longer consider the optimal algorithms in the rest of this section.

Comparisons between the efficient and baseline algorithms. We first report the performance results of the efficient and baseline algorithms in Figure 19. Figure 19(a) and 19(b) show that the proposed EFF$_{avg}$ and EFF$_{mm}$ achieve the design goals: (i) EFF$_{avg}$ leads to the highest average MOS scores and (ii) EFF$_{mm}$ results in the highest worst MOS scores. Moreover, they outperform the two baseline algorithms by up to 30% and 46%. Figure 19(c) reveals that EFF$_{avg}$ leads to higher efficiency than EFF$_{mm}$, but both of them outperform the baseline algorithms. Last, Figure 19(d) shows that when $U \geq 500$, all four algorithms allocate roughly equal bitrate to gamers. This indicates that the superior performance of our efficient algorithms is not built upon excessive resource consumption. We take a closer look by reporting the link utilization in Figure 20. Figure 20(a) reveals that our efficient algorithms lead to gamer link utilization no larger than that of the baseline algorithms. Furthermore, more gamers result in lower gamer link utilization, indicating that the bottleneck is at the data center. This is confirmed by Figure 20(b): the data center link utilization reaches 100% when there are more than 500 gamers. Another observation on Figure 20 is that no algorithm overloads the links, which illustrates the correctness of our algorithm design and simulator implementation.

Difference between EFF$_{avg}$ and EFF$_{mm}$. The two efficient algorithms target different optimization criteria, and are optimal in terms of mean MOS scores and minimum MOS scores, respectively. We plot the average MOS scores of individual games in Figure 21. Figure 21(a) shows that with EFF$_{avg}$, the gamers playing Batman achieve higher MOS scores, which can be attributed to the optimization criterion:

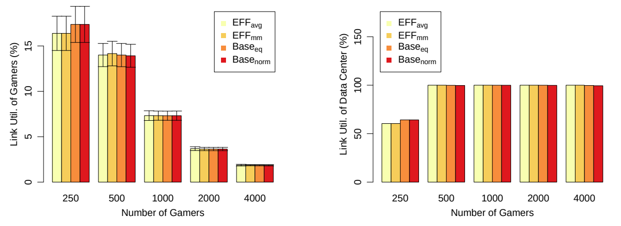
(a) (b)

Fig. 20. Link utilization: (a) across all gamers and (b) of the data center under different adaptation algorithms.

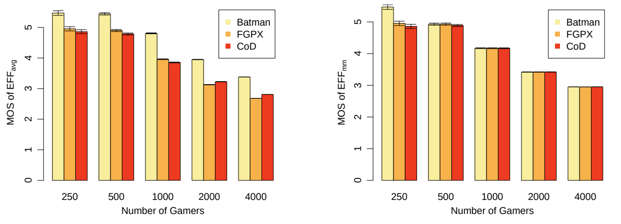
(a) (b)

Fig. 21. Mean MOS scores under different numbers of gamers using two adaptation algorithms: (a) EFF$_{avg}$ and (b) EFF$_{mm}$.

investing bandwidth on Batman leads to higher improvement on the MOS scores. In contrast, Figure 21(b) demonstrates that EFF$_{mm}$ indeed achieves fairness on the MOS scores: gamers playing all three games achieve the same MOS score except when $U = 250$. A closer look (cf. Figure 20(b)) indicates that when there are fewer gamers, there are actually more than enough bandwidth for all gamers to achieve the highest MOS scores. This demonstrates that our EFF$_{mm}$ algorithm is designed in a way that it does not only maintain fairness, but also capitalize all the available resources.

Implication of different data center available bandwidth. We report the MOS scores under different values of $R \in \{0.5R, 1R, 2R, 4R\}$ in Figure 22. It shows that higher available bandwidth leads to smaller gap between our efficient algorithms and the baseline algorithms. This can be explained by Figure 22(b). It shows that higher available bandwidth results in low data center link utilization. More specifically, when the data center bandwidth increases, gamers' links become the bottlenecks. This reduces the optimization room of our algorithms, and results in smaller gaps.

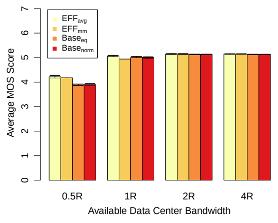

(a)

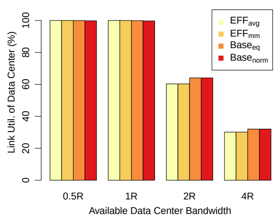

(b)

Fig. 22. Impacts of different available bandwidth R: (a) average MOS scores and (b) data center link utilization.

Our efficient algorithms scale to large problems. To verify the scalability of our efficient algorithms, we measure the running time of the EFF$_{avg}$ and EFF$_{mm}$ algorithms under various number of gamers. We report the average running time in Table VI, which shows that it takes at most ~ 1.7 seconds to solve an adaptation problem with more than 8000 gamers, showing that the efficient algorithms scale to large cloud gaming platforms.

TABLE VI
Running Time in Seconds

# of Gamers	EFF$_{avg}$		EFF$_{mm}$	
	Mean	Max	Mean	Max
500	0.181	0.183	0.179	0.184
1000	0.296	0.299	0.287	0.290
2000	0.523	0.531	0.520	0.533
4000	1.000	1.104	1.060	1.066
8000	1.677	1.681	1.654	1.661

VIII. Conclusion

In this paper, we studied the problem of adapting cloud gaming sessions to maximize the gamer experience in dynamic environments in three steps. First, we conducted a crowdsourcing-based user study to measure and model the gamer experience under different video codec configurations. Second, we enhanced GA, an open-source cloud gaming platform to support video codec reconfigurations, which allows the cloud gaming platform to adapt the frame rate and bitrate of each cloud gaming session on-the-fly. Third, with the gamer experience model and adaptation mechanism, we presented two formulations with different optimization criteria of: (i) maximizing the average MOS scores across all gamers and (ii) maximizing the minimum MOS scores among all gamers. We then proposed two optimal and two efficient algorithms to solve these two adaptation problems. We analytically showed that the proposed efficient algorithms run in polynomial time, yet achieve optimal adaptations. We carried out extensive trace-driven simulations, and the simulation results comply with our analysis. In addition, the proposed efficient algorithms: (i) outperform the baseline algorithms by up to 46% and 30%, (ii) run fast and scale to large ($\geq$ 8000 gamers) problems, and (iii) indeed achieve the user-specified optimization criteria. The enhanced cloud gaming platforms will be made publicly available, which can be leveraged by many researchers, developers, and gamers.

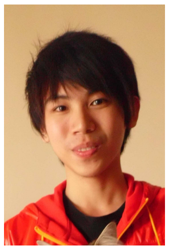

Hua-Jun Hong Hua-Jun Hong is a PhD student at the National Tsing Hua University, Taiwan. He received his B.S. and M.S. in Computer Science from National Tsing Hua University. His research interests are in cloud computing, cloud gaming, and multimedia networking.

Chih-Fan Hsu is a research assistant in Academia Sinica from 2014, and began the pursue of his Ph.D. in Department of Electrical Engineering of National Taiwan University since 2015. His research interests cover computer vision, camera calibration, and quality of experience.

Tsung-Han Tsai received his master degree in Computer Science and Information Engineering from National Chiayi University, Taiwan, in 2013. He joined Academia Sinica in 2013 as a research assistant. His research interest includes multimedia systems and social computing.

Chun-Ying Huang (S'03–M'08) is an Associate Professor at the Department of Computer Science and Engineering, National Taiwan Ocean University. He received his B.S. in Computer Science from National Taiwan Ocean University in 2000 and M.S. in Computer Information Science from National Chiao Tung University in 2002. Dr. Huang received his Ph.D. in Electrical Engineering Department from National Taiwan University in 2007. His researches focus on computer network and network security issues, including traffic measurement and analysis, malicious behavior detection, and multimedia networking systems. Dr. Huang is a member of ACM, CCISA, IEEE, and IICM.

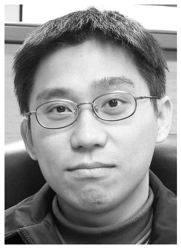

Kuan-Ta Chen (a.k.a. Sheng-Wei Chen) (S'04–M'06–SM'15) is a Research Fellow at the Institute of Information Science and the Research Center for Information Technology Innovation (joint appointment) of Academia Sinica. Dr. Chen received his Ph.D. in Electrical Engineering from National Taiwan University in 2006, and received his B.S. and M.S. in Computer Science from National Tsing-Hua University in 1998 and 2000, respectively. His research interests include quality of experience, multimedia systems, and social computing. He has been an Associate Editor of *ACM Transactions on Multimedia Computing, Communications, and Applications (TOMM)* since 2015. He is a Senior Member of ACM and a Senior Member of IEEE.

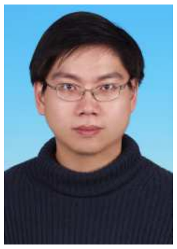

Cheng-Hsin Hsu (S'09–M'10) received the B.Sc. degree in mathematics and M.Sc. degree in computer science and information engineering from National Chung-Cheng University, Taiwan, in 1996 and 2000, respectively. He received the M.Eng. degree in electrical and computer engineering from the University of Maryland, College Park, in 2003 and the Ph.D. degree in computing science from Simon Fraser University, Burnaby, BC, Canada, in 2009. He is an associate professor at National Tsing Hua University at Hsin Chu, Taiwan. His research interests are in the area of multimedia networking and distributed systems. He is a member of the IEEE and ACM.

References

[1] "Why cloud hosting is the future of online gaming," April 2014, http://www.developer-tech.com/news/2014/apr/15/why-cloud-hosting-future-online-gaming2/.

[2] "OnLive web page," July 2014, http://www.onlive.com/.

[3] "GaiKai web page," July 2014, http://www.gaikai.com/.

[4] "Ubitus web page," July 2014, http://www.ubitus.net.

[5] "Internap online gaming," July 2014, http://www.internap.com/solutions/industry/online-gaming/.

[6] K.-T. Chen, C.-Y. Huang, and C.-H. Hsu, "Cloud gaming onward: Research opportunities and outlook," in *Proceedings of IEEE C-Game 2014*, 2014.

[7] Y.-T. Lee, K.-T. Chen, H.-I. Su, and C.-L. Lei, "Are all games equally cloud-gaming-friendly? an electromyographic approach," in *Proceedings of IEEE/ACM NetGames 2012*, Oct 2012.

[8] K.-T. Chen, Y.-C. Chang, H.-J. Hsu, D.-Y. Chen, C.-Y. Huang, and C.-H. Hsu, "On the quality of service of cloud gaming systems," *IEEE Transactions on Multimedia*, Feb 2014.

[9] H.-J. Hong, D.-Y. Chen, C.-Y. Huang, K.-T. Chen, and C.-H. Hsu, "Placing virtual machines to optimize cloud gaming experience," *IEEE Transactions on Cloud Computing*, Jan 2015.

[10] M. Claypool, D. Finkel, A. Grant, and M. Solano, "Thin to win? network performance analysis of the onlive thin client game system," in *Proc. of ACM Annual Workshop on Network and Systems Support for Games (NetGames'12)*, Venice, Italy, October 2012.

[11] "GamingAnywhere: An open source cloud gaming project," 2013, http://gaminganywhere.org.

[12] C.-Y. Huang, K.-T. Chen, D.-Y. Chen, H.-J. Hsu, and C.-H. Hsu, "GamingAnywhere: The first open source cloud gaming system," *ACM Transactions on Multimedia Computing Communications and Applications*, pp. 1–25, Jan 2014.

[13] P. Eisert and P. Fechteler, "Low delay streaming of computer graphics," in *Proc. of IEEE International Conference on Image Processing (ICIP'08)*, San Diego, CA, October 2008, pp. 2704–2707.

[14] A. Jurgelionis, P. Fechteler, P. Eisert, F. Bellotti, H. David, J. Laulajainen, R. Carmichael, V. Poulopoulos, A. Laikari, P. Perala, A. Gloria, and C. Bouras, "Platform for distributed 3D gaming," *International Journal of Computer Games Technology*, vol. 2009, pp. 1:1–1:15, January 2009.

[15] S. Shi, C. Hsu, K. Nahrstedt, and R. Campbell, "Using graphics rendering contexts to enhance the real-time video coding for mobile cloud gaming," in *Proc. of ACM Multimedia (MM'11)*, Scottsdale, AZ, November 2011, pp. 103–112.

[16] F. Giesen, R. Schnabel, and R. Klein, "Augmented compression for server-side rendering," in *Proc. of International Fall Workshop on Vision, Modeling, and Visualization (VMV'08)*, Konstanz, Germany, October 2008.

[17] Y. Chen, C. Chang, and W. Ma, "Asynchronous rendering," in *Proc. of ACM SIGGRAPH symposium on Interactive 3D Graphics and Games (I3D'10)*, Washington, DC, February 2010.

[18] D. Winter, P. Simoens, L. Deboosere, F. Turck, J. Moreau, B. Dhoedt, and P. Demeester, "A hybrid thin-client protocol for multimedia streaming and interactive gaming applications," in *Proc. of ACM International Workshop on Network and Operating Systems Support for Digital Audio and Vid eo (NOSSDAV'06)*, Newport, RI, May 2006.

[19] O. Holthe, O. Mogstad, and L. Ronningen, "Geelix LiveGames: Remote playing of video games," in *Proc. of IEEE Consumer Communications and Networking Conference (CCNC'09)*, Las Vegas, NV, January 2009.

[20] C.-Y. Huang, C.-H. Hsu, D.-Y. Chen, and K.-T. Chen, "Quantifying user satisfaction in mobile cloud games," in *Proceedings of ACM MoVid 2014*, 2014.

[21] C.-Y. Huang, L.-L. Huang, Y.-H. Chi, K.-T. Chen, and C.-H. Hsu, "To cloud or not to cloud: Measuring the performance of mobile gaming," in *Proceedings of ACM MobiGames 2015*, May 2015.

[22] I. Ghergulescu, A.-N. Moldovan, and C. Muntean, "Energy-aware adaptive multimedia for game-based e-learning," in *IEEE International Symposium on Broadband Multimedia Systems and Broadcasting (BMSB'14)*, June 2014, pp. 1–6.

[23] H.-J. Hong, T.-Y. Fan-Chiang, C.-R. Lee, K.-T. Chen, C.-Y. Huang, and C.-H. Hsu, "GPU consolidation for cloud games: Are we there yet?" in *Proceedings of IEEE/ACM NetGames 2014*, 2014.

[24] Y.-T. Lee and K.-T. Chen, "Is server consolidation beneficial to MMORPG? a case study of World of Warcraft," in *Proc. of IEEE CLOUD 2010*, February 2010.

[25] T. Duong, X. Li, R. Goh, X. Tang, and W. Cai, "QoS-aware revenue-cost optimization for latency-sensitive services in IaaS clouds," in *Proc. of IEEE/ACM 16th International Symposium on Distributed Simulation and Real Time Applications (DS-RT'12)*, Dublin, Ireland, October 2012.

[26] D. Wu, Z. Xue, and J. He, "iCloudAccess: Cost-effective streaming of video games from the cloud with low latency," *IEEE Transactions on Circuits and Systems for Video Technology*, January 2014, accepted to appear.

[27] S. Wang and S. Dey, "Rendering adaptation to address communication and computation constraints in cloud mobile gaming," in *Proc. of IEEE Global Telecommunications Conference (GLOBECOM'10)*, 2010.

[28] W. Cai, M. Chen, and V. Leung, "Towards gaming as a service," *IEEE Transactions on Internet Computing*, vol. 18, no. 3, pp. 12–18, May 2014.

[29] S. Wang and S. Dey, "Modeling and characterizing user experience in a cloud server based mobile gaming approach," in *Proc. of IEEE Global Telecommunications Conference (GLOBECOM'09)*, December 2009.

[30] ——, "Cloud mobile gaming: Modeling and measuring user experience in mobile wireless networks," *ACM Transactions on Mobile Computing and Communications Review*, vol. 16, no. 1, pp. 10–21, January 2012.

[31] Y. Xu and S. Mao, "A survey of mobile cloud computing for rich media applications," *IEEE Transactions on Wireless Communications*, vol. 20, no. 3, pp. 46–53, June 2013.

[32] L. Lozano, E. Garcia-Cueto, and J. Muniz, "Effect of the number of response categories on the reliability and validity of rating scales," *European Journal of Research Methods for the Behavioral and Social Sciences*, vol. 4, no. 2, pp. 73–79, 2008.

[33] C.-Y. Huang, C.-H. Hsu, D.-Y. Chen, and K.-T. Chen, "Quantifying user satisfaction in mobile cloud games," in *Proc. of ACM Workshop on Mobile Video Delivery (MoVid'14)*, March 2014, pp. 4:1–4:6.

[34] M. Li, M. Claypool, and R. Kinicki, "Wbest: a bandwidth estimation tool for ieee 802.11 wireless networks," in *Proc. of IEEE Conference on Local Computer Networks (LCN'08)*, Montreal, Canada, Oct 2008, pp. 374–381.

[35] V. Ribeiro, R. Riedi, R. Baraniuk, J. Navratil, and L. Cottrell, "Pathchirp: Efficient available bandwidth estimation for network paths," in *Proc. of Passive and Active Monitoring Workshop (PAM'03)*, vol. 4, San Diego, CA, Apr 2003.

[36] R. Kapoor, L. Chen, L. Lao, M. Gerla, and M. Y. Sanadidi, "Capprobe: A simple and accurate capacity estimation technique," in *Proc. of SIGCOMM'04*, Portland, OR, Aug 2004, pp. 67–78.

[37] Y. Wang, J. Ostermann, and Y. Zhang, *Video Processing and Communications*. Prentice Hall, 2001.

[38] "IBM ILOG CPLEX optimizer," http://www-01.ibm.com/software/integration/optimization/cplex-optimizer/.

[39] "NetIndex real time global broadband and mobile data," http://www.netindex.com/.